Research in Nondestructive Evaluation, 16: 55–64, 2005

ISSN: 0934-9847 print /1432-2110 online
DOI: 10.1080/09349840591003212

Taylor & Francis
Taylor & Francis Group

DETECTION OF FIBER DIRECTION IN COMPOSITES BY MEANS OF A HIGH-FREQUENCY WIDE-BOUNDED ULTRASONIC BEAM AND SCHLIEREN PHOTOGRAPHY

Nico F. Declercq,[1] A. Teklu,[1] M. A. Breazeale,[1] Roger D. Hasse,[1] Joris Degrieck[2], and Oswald Leroy[2]

[1]National Center for Physical Acoustics, University of Mississippi, Oxford, MS, USA
[2]Soete Laboratory, Department of Mechanical Construction and Production, Ghent University, Ghent, Belgium

This work describes an experimental method, based on the combination of schlieren photography and a 2.5-cm-wide-bounded ultrasonic beam of 10 MHz, used to detect the fiber direction in composites. Experiments are described on unidirectional and fabric fiber-reinforced composites. The method exploits the spatially dependent reflection coefficient because of discontinuities in the fiber density. The typical discontinuities that reflect the fiber direction are detectable if 10-MHz ultrasound is applied. Lower frequencies are not susceptible to these typical discontinuities, whereas larger frequencies would make the use of schlieren photography more difficult.

Keywords: Alignment, composites, defects, fiber direction, schlieren photography, ultrasound

INTRODUCTION

Because fiber-reinforced composites are mostly tuned to decrease their weight and to get the necessary stiffness in certain vital directions, it is important to know the fiber direction at any time during the construction or maintenance processes. The impact response, fatigue damage, and stiffness all depend upon the direction [1–5]. There are methods available to assess the fiber direction, such as ultrasonic polar scans [6–9] or ultrasonic reflected bounded beam deformation properties [10]. These methods are based on the Lamb wave phenomena and the direction-dependent mechanical properties of the composite. The applied frequencies are relatively low (1–5 MHz). At low frequencies, ultrasound is not susceptible to typical microscopic inhomogeneities such as infividual fibers or bunches of fibers. Therefore, only the mean properties of composites are felt, and the composite can be considered homogeneous at those frequencies. Other possible techniques are optical micrography [11] or Moiré interferometry [12]. Such techniques

Address correspondence to Nico F. Declercq, Soete Laboratory, Department of Mechanical Construction and Production, Ghent University, Sint Pietersnieuwstraat 41, B-9000 Ghent, Belgium. E-mail: NicoF.Declercq@UGent.be

mainly characterize the surface-layer fiber direction and are actually best applied when some of the fibers are exposed after polishing the sample of interest.

The technique described here is based on the interaction of relatively high-frequency sound (10 MHz) with the composite under investigation. It exploits imperfections [13–15] in the fiber density of the fiber-reinforced layers relatively close to the surface. These imperfections are formed in regions where sharp transitions from high to low fiber density is observed. Such inhomogeneities, resulting in a spatially dependent reflection coefficient, are detected with the more sensitive high-frequency sound. If, in addition, a relatively wide beam is used (wider than the imperfections), the reflected-beam profile will be fringed because of the spatially dependent reflection coefficient. This fringing will be there for any type of imperfection that is smaller than the width of the applied bounded ultrasonic beam. However, for imperfections along the fiber direction, such as spatial fiber-density variations, which normally span several millimeters or centimeters parallel to the fibers, the fringes will cleave the reflected sound beam along the fiber direction. Hence, when schlieren photography [16] is used to visualize the reflected beam, the fringing will be visible on the schlieren picture as a pattern of high-intensity light alternated with low-intensity light. Contrary to reflected-beam spatial-intensity patterns when the frequency is low (1–5 MHz), which are the result of a form of the Schoch effect caused by multilayer Lamb waves or Rayleigh waves [10], the pattern described here is independent of the angle of incidence and is solely a result of inhomogeneities near the surface.

EXPERIMENTAL CONFIGURATION AND PROCEDURE

Schlieren photography is based on the diffraction of light by ultrasound and is well described in Ref. 16. A monochromatic schlieren experimental setup is used as shown in Fig. 1. Two large (f/6.3, 1.2192-m focal length) lenses are used (L2 and L3). A monochromatic laser-light beam generated by a 10-mW He-Ne laser source is focused by the first lens L1 onto a pinhole that is placed exactly at 1.2192 m of L2. After passage through L2, the light is collimated to get a perfect parallel wide laser beam passing through the water tank. This light beam is then focused by L3 on a spatial filter that blocks all undiffracted light. Therefore, only diffracted light reaches the projection screen, and visualization of ultrasound is achieved. The image is then captured by a digital camera and stored on a computer.

A 2.5-cm wide ultrasonic beam of 10 MHz impinges the surface of the sample under investigation. This angle is not crucial; as a matter of fact, it is randomly chosen (33°) and the results shown are valid for each angle of incidence. Figure 2 shows the acoustic beam of a 10-MHz 2.5-cm transducer reflecting from an aluminum block.

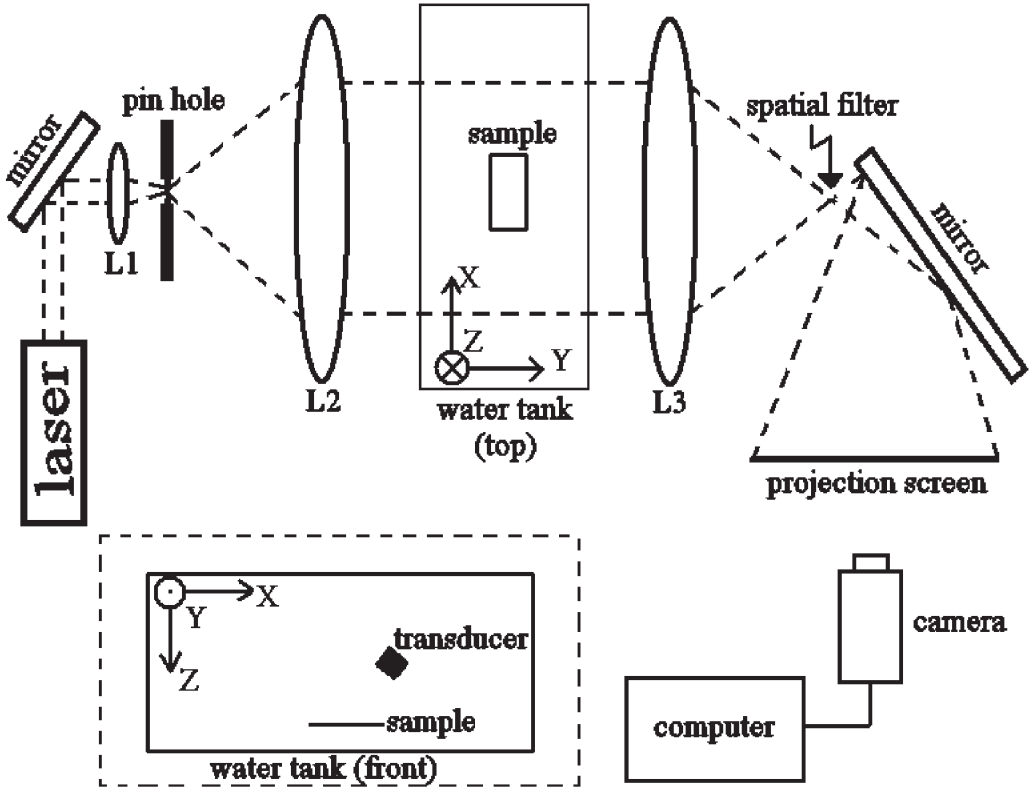

FIGURE 1. Schematic of the experimental configuration. ''L'' stands for lens.

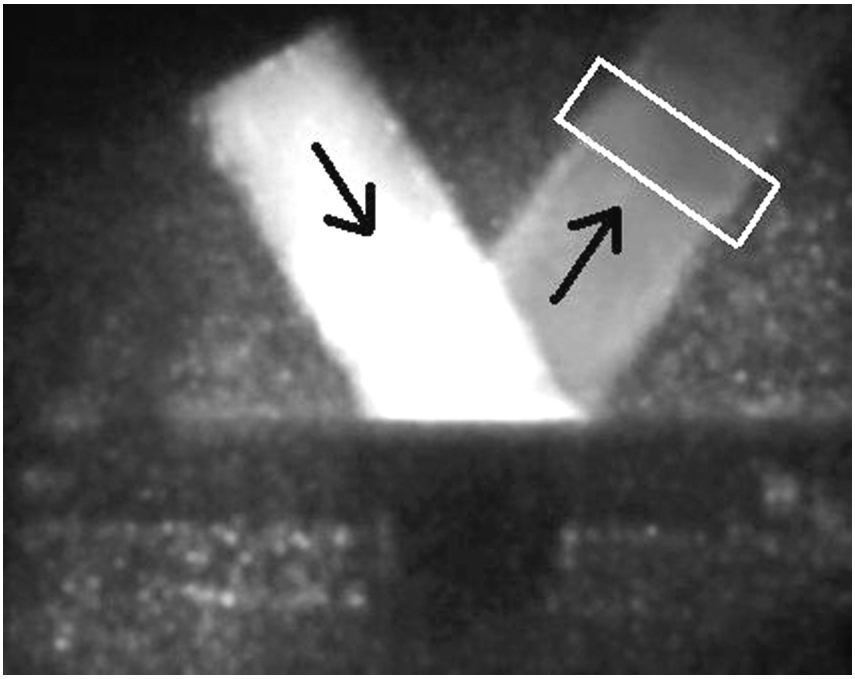

FIGURE 2. 2.5-cm-wide 10-MHz ultrasonic beam incident and reflected on an aluminum block. From the visualized reflected beam we always extract the area on the picture denoted by the white rectangle for studying the reflected-beam pattern.

Although the amplitude of the reflected beam is smaller than the incident beam, it retains the Gaussian distribution as shown in Fig. 3.

Figure 3 serves as a reference for all results obtained in this study. Figure 2 is a monochromatic schlieren photograph of the incident and reflected ultrasound beam. The laser light that is used to obtain this image is shined normal to the plane of the ultrasonic beam propagation. In what follows, the path between L_2 and L_3 is referred to as the laser-light direction. In all experiments the samples under consideration are placed on a highly ultrasound-absorbing material to prevent side effects coming from reflections on the base where the samples are positioned.

FIGURE 3. Reflected-beam pattern for an aluminum sample. No fringes are visible.

FIGURE 4. Reflected-beam pattern for a carbon-epoxy unidirectional composite.

FIGURE 5. Reflected-beam pattern for a glass-epoxy unidirectional composite.

RESULTS AND DISCUSSION

Unidirectional Carbon-Fiber-Reinforced Epoxy and Glass-Fiber-Reinforced Epoxy

If a unidirectional carbon-fiber-reinforced epoxy laminate is placed in the experimental setup of Fig. 2, there is always a pattern visible as shown in Figs. 2 and 3, except for the case when the laser light is parallel to the fiber direction, which generates a pattern as shown in Fig. 4. Equal findings hold for a unidirectional glass-fiber-reinforced epoxy, as shown in Fig. 5. Notice that the fibers in both samples are not perfectly parallel to each other. This is attributed to spatial variations in fiber density caused by imperfect preimpregnated fibers and caused by the fabrication process. A pattern as shown in Figs. 4 and 5 is possible. The reason is described in the previous paragraph.

Unidirectional ($[0^\circ]_8$) Stacked Four-Harness Glass-Fabric-Reinforced Epoxy and Crossply ($[0^\circ/90^\circ]_{2s}$) Stacked Glass-Fabric-Reinforced Epoxy

$[0^\circ]_8$ stacking means that eight layers are stacked as $[0^\circ/0^\circ/0^\circ/0^\circ/0^\circ/0^\circ/0^\circ/0^\circ]$. $[0^\circ/90^\circ]_{2s}$ stacking means that eight layers are stacked as $[0^\circ/90^\circ/0^\circ/90^\circ/90^\circ/0^\circ/90^\circ/0^\circ]$. The angles in both definitions are the in-plane directions of the fibers.

The patterns of Figs. 4 and 5 (especially the one of Fig. 5) do not show spectacular differences when compared with Fig. 3. That is of course because the pattern is based on small density variations. However, in practical applications pure unidirectional materials are seldom used, whereas many kinds of fabrics are much more common. In Fig. 6 a photograph is shown of the type of fabric that is often used for the same purposes as a

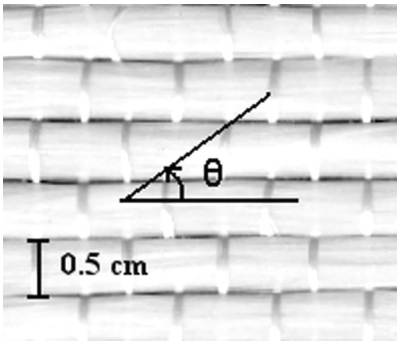

FIGURE 6. Photograph of the fibers that are used in manufacturing the unidirectional glass-fabric-reinforced epoxy samples. The width of the warp bunches (horizontal) is 5 mm. The angle θ is shown and corresponds to the angles denoted in Figs. 7 and 8.

purely unidirectional material. Most of the fibers (in bunches) in Fig. 6 are directed along the 0° direction. However, to hold them together, a small number of fibers are woven in the 90° direction. This does not result in different stiffness properties when compared to a purely unidirectional material. It is commonly found in a typical layup fabrication process. Nevertheless, the presence of weft fibers (90°) results in the formation of bunches of fibers, instead of pure homogeneously distributed fibers in the 0° direction. Using the described schlieren technique to ascertain the fiber direction is appealing for this phenomenon. Experiments are performed on unidirectional $([0^\circ]_8)$ stacked glass-fabric-reinforced epoxy and have shown that the reflected-beam profile is always equal to Fig. 3, except when the laser light direction θ (see Fig. 6) is equal to 0°, 45°, or 90°, as can be seen in Fig. 7. If the direction is 0°, bunches of fibers are present. If the direction is 90°, spatial separation of the weft fiber bunches is present. If the direction is 45°, this is also a symmetry direction for the fabric.

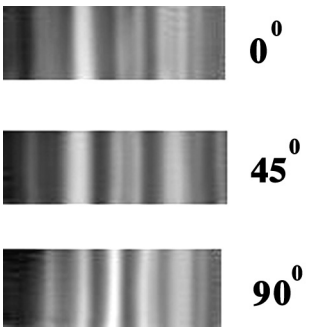

FIGURE 7. Reflected-beam pattern for a $[0^\circ]_8$ stacked glass-epoxy laminate with layers reinforced with unidirectional composite such as in Fig. 5.

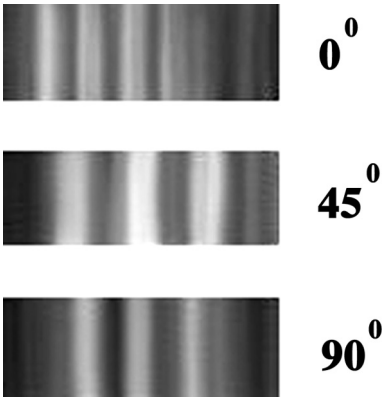

FIGURE 8. Reflected-beam pattern for a $[0°/90°]_{2s}$ stacked glass-epoxy laminate with layers reinforced with unidirectional composite such as in Fig. 5.

If the same experiment is repeated for crossply ($[0°/90°]_{2s}$) stacked glass-fabric-reinforced epoxy, then again no fringes are visible except if laser light is directed at 0°, 45°, or 90°, measured from the fiber direction for the upper layer. The results are shown in Fig. 8. The fact that the patterns in the 0° and 90° directions are approximately the same as far as the spacing between the fringes is concerned (which is not the case in Fig. 7) shows that the pattern is not just influenced by the properties of the upper layer, but also by lower layers in the composite sample. Ultrasound penetrates deep enough to be influenced by more than one layer. One of the consequences of this feature of the technique is that when the composite is covered by a coating (homogeneous and isotropic), the fringes will still be visible. The allowed thickness of the coating depends on its damping and acoustical impedance properties. As long as the coating does not prevent sound from reaching the layer underneath and returning to the surface, the technique as introduced here is applicable.

Unidirectional Five-Harness Satin-Weave Fabric ($[0°]_8$) Stacked and Crossply Five-Harness Satin-Weave Fabric ($[0°/90°]_{2s}$) Stacked Carbon-Fabric-Reinforced PPS

The previous section describes experiments on samples that consist of quasi-unidirectional fibers. That is because the weft bunches are much smaller than the warp bunches. In the aviation industry often real fabric layers are used, that is, layers where the weft and warp bunches have comparable size. For that reason we have also performed experiments on unidirectional five-harness satin-weave fabric ($[0°]_8$) stacked carbon-fabric-reinforced polyphenyl sulfide (PPS). A photograph is shown in Fig. 9. The directions 1 (–25°), 2 (0°), 3 (19°), and 4 (65°) correspond to symmetry directions of the composite that result in fringed patterns if the laser light

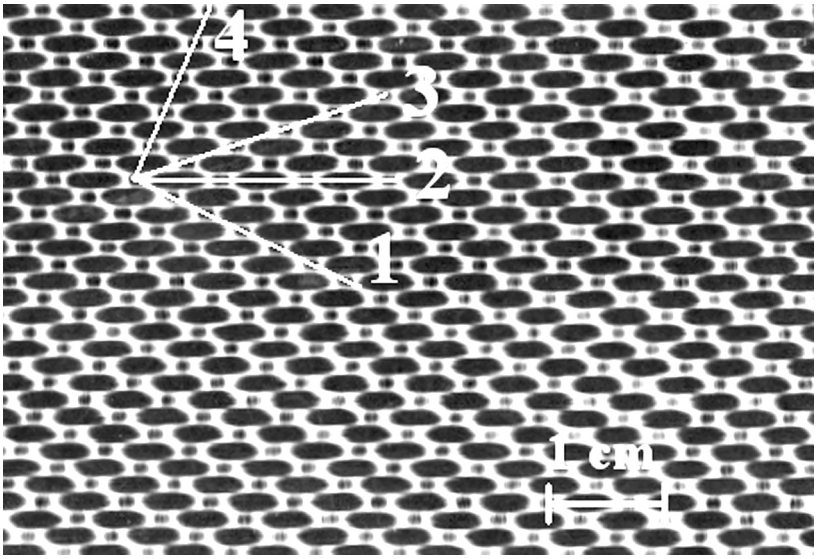

FIGURE 9. Definition of the direction 1 (–25°), 2 (0°), 3 (19°), and 4 (65°) on the upper surface of a PPS five-harness satin-weave-fabric carbon-fiber-reinforced composite.

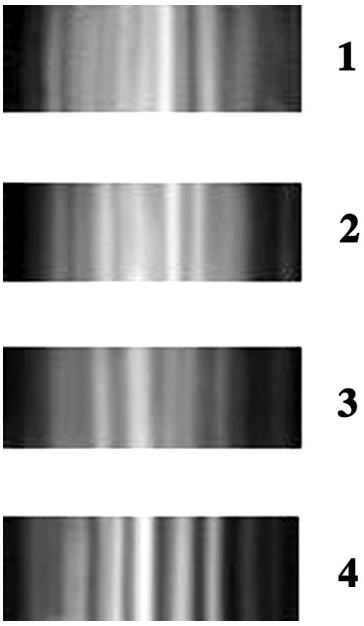

FIGURE 10. Reflected-beam pattern along the directions as defined in Fig. 9 for a $[0^\circ]_8$ stacked laminate with layers as described in Fig. 8. The upper layer has a direction equal to the layer shown photographically in Fig. 9.

FIGURE 11. Reflected-beam pattern along the directions as defined in Fig. 8 for a $[0^\circ/90^\circ]_{2s}$ stacked laminate with layers as described in Fig. 8. The upper layer has a direction equal to the layer shown photographically in Fig. 8.

is passed in those directions. The results are shown in Fig. 10 for each of those directions.

Because the symmetry for the pattern shown in Fig. 9 is quite different when compared to the symmetry observed in Fig. 6, it is expected that a composite consisting of a stack of such layers in 0° and 90° directions will cancel the effects of the outcome of each layer on reflected ultrasound. It is expected, therefore, that no fringes can be visible in directions labeled 4 and 1, because those directions form an angle of approximately 90° with one another. Indeed, in Fig. 11 the result is shown for direction 4 (a similar result was found for direction 1), for a crossply five-harness satin-weave fabric ($[0^\circ/90^\circ]_{2s}$) stacked carbon-fabric-reinforced PPS. In the directions 1 and 4, a fringe pattern is visible, although not as distinct as in Fig. 10. Such a fringed pattern is not detectable in directions 2 and 3.

CONCLUSIONS

This article shows that the use of a 2.5-cm-wide 10-MHz ultrasonic beam, combined with a schlieren photography experimental setup, enables the symmetry directions of a composite to be determined. This technique can be used to detect the fiber direction(s) in composites. Results are shown for different types of composites.

ACKNOWLEDGMENTS

This work was supported by a Collaborative Linkage Grant from NATO (PST.CLG.980315) and by The Flemish Institute for the Encouragement of the Scientific and Technological Research in Industry (I.W.T.).

REFERENCES

1. H. Fukunaga and G. N. Vanderplaats. Strength optimization of laminated composites with respect to layer thickness and/or layer orientation angle. *Computers and Structures* **40(6)**:1429–1439 (1991).
2. R. W. Rydin, A. Locurcio, and V. M. Karbhari. Influence of reinforcing layer orientation on impact response of plain weave RTM composites. *J. Reinforsed Plastics and Composites* **14(11)**:1199–1225 (1995).

3. O. S. Es-Said, J. Foyos, R. Noorani, M. Mendelson, R. Marloth, and B. A. Pregger. Effect of layer orientation on mechanical properties of rapid prototyped samples. *Materials and Manufacturing Processes* **15(1)**:107–122 (2000).
4. W. S. Lee, W. C. Sue, and S. T. Chiou. Effect of reinforcement orientation on the impact fracture of carbon fiber reinforced 7075-T6 aluminum matrix composite. *Materials Trans. JIM* **41(8)**:1055–1063 (2000).
5. T. Kurashiki, M. Zako, and I. Verpoest. Damage development of woven fabric composites considering an effect of mismatch of layup. *Proc. Tenth European Conf. on Composite Materials ECCM-10* (2002).
6. W. H. M. Vandreumel and J. L. Speijer. Polar-scan, a non-destructive test method for the inspection of layer orientation and stacking order in advanced fiber composites. *Materials Evaluation* **41(9)**:1060–1062 (1983).
7. J. Degrieck. Some Possibilities of Nondestructive Characterization of Composite Plates by Means of Ultrasonic Polar Scans. In *Non-Destructive Testing*, D. Van Hemelrijck and A. Anastassopoulos (eds.), pp. 225–236 (1996). Balkema, Rotterdam.
8. J. Degrieck, N. F. Declercq, and O. Leroy. Ultrasonic polar scans as a possible means of nondestructive testing and characterization of composite plates. *Insight—The Journal of the British Institute of Non-Destructive Testing* **45(3)**:196–201 (2003).
9. N. F. Declercq, J. Degrieck, and O. Leroy, Numerical Simulations of Ultrasonic Polar Scans. In *Emerging Technologies in Non-Destructive Testing*, D. Van Hemelrijck, A. Anastasopoulos, and N. E. Melanitis (eds.), pp. 75–80 (2004). Swets & Zeitlinger, Lisse.
10. A. U. Rehman, C. Potel, and J. F. de Belleval. Numerical modeling of the effects on reflected acoustic field for the changes in internal layer orientation of a composite. *Ultrasonics* **36(1–5)**:343–348 (1998).
11. C. J. Creighton, M. P. F. Sutcliffe, and T. W. Clyne. A multiple field image analysis procedure for characterisation of fibre alignment in composites. *Composites Part A—Applied Science and Manufacturing* **32(2)**:221–229 (2001).
12. R. D. Hale and D. O. Adams. Influence of in-plane fiber misalignment on moiré interferometry results. *J. Composite Materials* **31**(24):2444–2459 (1997).
13. J. Chen, T. M. McBride, and S. B. Sanchez. Sensitivity of mechanical properties to braid misalignment in triaxial braid composite panels. *J. Composite Technology & Research* **20(1)**:13–17 (1998).
14. A. Vincenti, P. Vannucci, and G. Verchery. Influence of orientation errors on quasi-homogeneity of composite laminates. *Composites Science and Technology* **63**:739–749 (2003).
15. S. C. Barwick and T. D. Papathanasiou. Identification of fiber misalignment in continuous fiber composites. *Polymer Composites* **24(3)**:475–486 (2003).
16. M. A. Breazeale. From monochromatic light diffraction to colour schlieren photography. *J. Opt. A: Pure Appl. Opt.* **3**:S1–S7 (2001).